

Effects of Additives on Coke Reactivity and Sulfur Transformation during Co-pyrolysis of Long Flame Coal and High-Sulfur Coking Coal

Wenguang Li, Yanfeng Shen, Jiang Guo, Jiao Kong, Meijun Wang,* and Liping Chang*

Cite This: *ACS Omega* 2021, 6, 34967–34976

Read Online

ACCESS |



Metrics & More

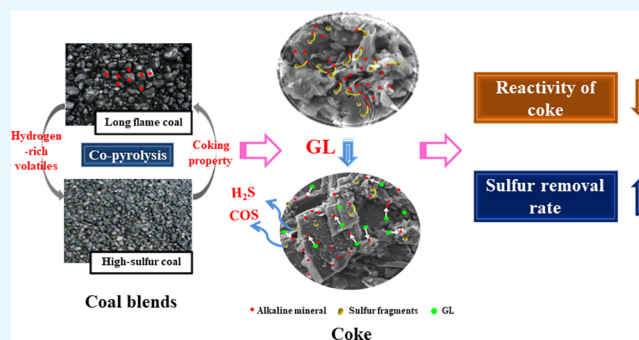


Article Recommendations



Supporting Information

ABSTRACT: A silica-aluminum-based mineral (GL) was selected for inspecting the effects of interactions of minerals in coal blends on the coke reactivity index (CRI) and sulfur transformation during co-pyrolysis of long flame coal and high-sulfur coking coal. Results indicate a good compatibility for the supply of active hydrogen, decomposition of sulfur, and regulation of reactivity. The experimental values of sulfur content in different coal blend cokes are lower than the calculated values, which can be determined as a result of the directional regulation effect of long flame coal on sulfur transformation. The addition of GL in coal blends significantly reduces the CRI of the corresponding coke, and the effect of GL on coke reactivity is also verified by a 10 kg coke oven experiment. When increasing the ratio of long flame coal, the sulfur fixation in the solid phase has a tendency to be enhanced by alkaline minerals. Also, GL plays a role in reducing the capture of sulfur free radicals by alkaline minerals, which improves the sulfur removal during pyrolysis of coal blends and then reduces the sulfur content in coke. This work provides a reference for using silica-aluminum-based minerals to reduce the capture of sulfur and catalytic effect on coke reactivity.



When increasing the ratio of long flame coal, the sulfur fixation in the solid phase has a tendency to be enhanced by alkaline minerals. Also, GL plays a role in reducing the capture of sulfur free radicals by alkaline minerals, which improves the sulfur removal during pyrolysis of coal blends and then reduces the sulfur content in coke. This work provides a reference for using silica-aluminum-based minerals to reduce the capture of sulfur and catalytic effect on coke reactivity.

1. INTRODUCTION

Metallurgical coke is an essential raw material for iron production. With the upsizing of blast furnaces and development of advanced coal injection technology, the requirement for coke quality has been enhancing. The thermal properties and sulfur content are quite important factors affecting the coke quality. With the continuous consumption of high-quality coking coals, the reserves are constantly decreasing and their prices are obviously higher than other kinds of coals. Furthermore, the reserve of high-volatile coal in China is relatively higher, but its utilization in the coking process is limited due to the lack of caking property. High-sulfur coking coal has suitable caking properties, but the higher sulfur content also restricts its ratio in coal blends. To achieve a high blending ratio of high-sulfur coking coal, Shen et al.¹ proposed to use abundant hydrogen-rich volatiles generated from high-volatile coal to regulate the sulfur transformation behavior during pyrolysis of high-sulfur coal. Therefore, it is feasible to blend long flame coal with high-sulfur coking coal to expand the coal resources used in the coking process and reduce the coking cost.

However, long flame coal generally has a much lower degree of metamorphism and contains active alkaline minerals that will deteriorate the thermal properties of coke.^{2,3} Suzuki et al.⁴ found that the concentrations of K and Na affected the catalytic effects on coke dissolution loss reaction, and these minerals contained in coke could form severe alkali circles that would further affect the stable operation in blast furnace.⁵ In

addition, alkaline minerals could capture sulfur-containing free radicals and affect the removal of sulfur in coal blends during the coking process.^{6,7} For the current layer-by-layer coking process in a coke oven, the generated sulfur-containing volatiles pass through the condensed plastic layer and coke layer that has a higher temperature, which further intensifies the volatiles' reaction with organic matter and minerals, likely resulting in more sulfur retention in the coke. In view of this, the authors previously conducted a heavy-liquid separation experiment of high volatile long flame coal to remove some alkaline minerals and enrich the high-volatile fractions, the effect on coke reactivity (CRI) could be reduced and the sulfur removal rate could be significantly improved during the co-pyrolysis with high-sulfur coal.⁸ It showed that the alkaline minerals in long flame coal were an important factor in the degradation of coke thermal properties.^{9–11} Therefore, the study on weakening the catalytic effect of alkaline minerals on coke reactivity and reducing the sulfur capture by minerals through regulating the interactions among long flame coal,

Received: October 9, 2021

Accepted: November 26, 2021

Published: December 8, 2021



high-sulfur coal, and minerals in coal blends during co-pyrolysis should raise more attention.

The conversions of alkaline minerals with different occurrence forms are significantly various during the pyrolysis process.^{12–14} Wang et al.¹⁵ found that the alkali metal and alkaline earth metal catalysts added in the coke could react with silica-aluminate minerals during the gasification process to generate silicate and silica-aluminate, resulting in a weak catalytic activity of alkaline minerals. Therefore, it is possible to weaken their catalytic effect on coke reactivity and capture of sulfur-containing free radicals by adjusting the interaction of minerals in coal blends and converting some alkaline minerals into a more stable state. It has been shown that silica-aluminum-based minerals in coal have a good trapping effect on alkaline minerals, which can be converted into silica-aluminate with high thermal stability.^{16–21} Gornostayev et al.²² proposed that some fine quartz could be added to the blast furnace to reduce the catalytic effect of alkali cycle on coke reactivity until the temperature reached about 2000 °C. However, the current studies on the influences of existing forms of alkaline minerals in coal blends on coke reactivity and sulfur transformation during co-pyrolysis of long flame coal and high-sulfur coking coal are still lacking.

In this work, a long flame coal is subjected to heavy liquid separation, the obtained fraction with a density less than 1.35 g/cm³ is selected as MF and high-sulfur coking coal is selected as the main components of coal blends. A silica-aluminum-based mineral (GL), which is ubiquitous in coal, is used as an additive to study the effects of the interaction of minerals in coal blends on the sulfur content and reactivity of coke. This research will provide guidance for the efficient utilization of long flame coal and high-sulfur coking coal and a feasible cost reduction method in the coking process.

2. RESULTS AND DISCUSSION

2.1. Effect of GL on Coke Reactivity. The reactivity results of coke obtained by pyrolysis with different proportions of GL are shown in Figure 1. It can be seen that the coke reactivity decreases with the increasing GL proportion, and it reaches the lowest value when the ratio of GL is 0.7%. However, the CRI is slightly higher after adding 1% GL. These results illustrate that the addition of GL is beneficial to reduce the CRI of coke, but the ratio of GL in coal blends should be limited. From Table 4, the alkaline minerals in MF are much

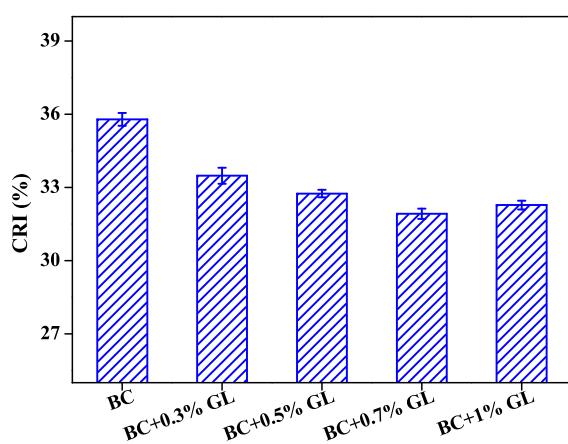


Figure 1. CRI of coke from pyrolysis of BC with different proportions of GL.

higher, and thus when the GL addition is lower, GL can bind with these alkaline minerals and weaken their catalytic effect on coke reactivity.²³ However, with the further addition of GL, as an inert mineral, it may affect the microcrystalline structure and pore structure of the coke. Also, since the difference in volume between the mineral and organic matter during pyrolysis is changed, some cracks may be formed, which will lead to the deterioration of mechanical strength of coke.²²

It is well known that the CRI of coke is related to many factors. Therefore, to determine the effect mechanism of GL addition on the gasification reaction, the carbon structure, pore structure, and minerals of coke are further investigated.

2.1.1. Influence of GL on the Coke Microcrystalline Structure and Porosity. The edge of the coke microcrystal belongs to the defect site of the crystal lattice, which can form unsaturated chemical bonds easily by combining heteroatoms, and becomes the active center during gasification reaction to promote the gasification activity. Therefore, the microcrystalline structure of coke is an important factor affecting coke reactivity.²⁴ Figure 2 shows the XRD spectra of coke obtained

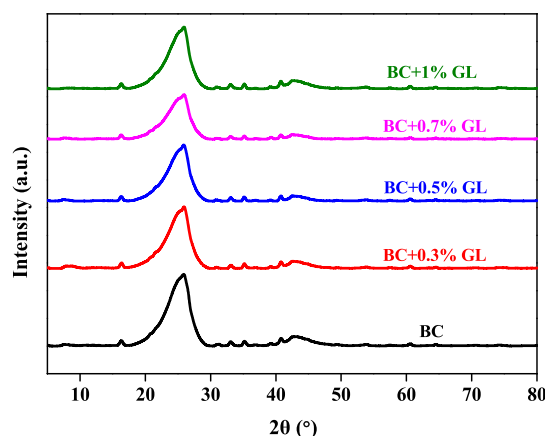


Figure 2. XRD of coke from pyrolysis of BC with different proportions of GL.

from coal blends with different proportions of GL. The addition of GL weakens the peak intensities of 002 and 100, which represent the size and orientation of the carbon reticulum layer in the aromatic ring of coke, respectively.²⁵ This indicates that the order degree of the microcrystalline structure of coke decreases and defect sites increase.²⁶ According to the mesophase coking theory, better growth of the intermediate phase is conducive to the higher order of coke microcrystalline structure. However, the addition of GL will cause intermolecular attraction and hinder the migration of the aromatic sheet, which is against the growth of the mesophase. In addition, GL could insert into the interlayer of aromatic lamellar deposits, distorting the lamellar deposits and destroying their order.²⁷ Thus, the addition of GL should increase the reactivity of coke,²⁶ which is contrary to the conclusion in Figure 1. This indicates that the catalytic effect of alkaline mineral on reactivity is greater than the effect of GL on the coke microcrystalline structure in the gasification process.

As a porous solid, the pore structure of coke is the key factor affecting the reaction rate of CO₂ gasification. In the gasification process, CO₂ diffuses into the pore structure of coke and gasification reaction occurs when it comes into contact with the active center on the pore surface.^{28,29} Therefore, the better-developed pore structure will cause a

more sufficient gas–solid contact and easier gasification reaction. Figure 3 shows the porosity of coke obtained after

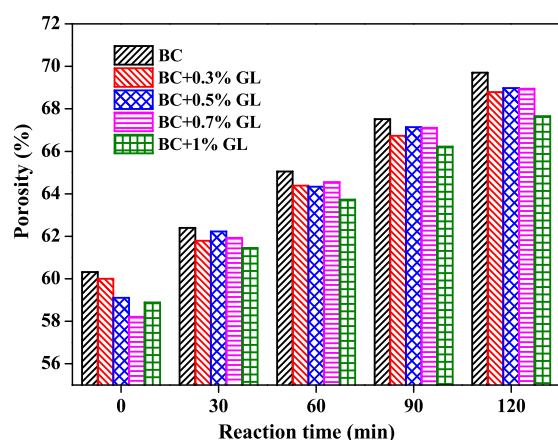


Figure 3. Porosity of coke obtained after the CO₂ gasification reaction at 1100 °C.

the CO₂ gasification reaction at 1100 °C. With the extension of the gasification reaction time, the porosity of coke gradually increases.^{30,31} The addition of GL slightly decreases the coke porosity after gasification. From the results shown in Table 4, MF contains a large amount of Ca, which can form channels at the active point of the calcium–carbon interface and generate pores.³² The addition of GL will combine with Ca and form a stable state retained in coke, weakening the pore-forming effect of Ca.

2.1.2. Capture Effect of GL on Alkaline Minerals. To verify the influence of the interaction between GL and alkaline minerals on the CRI of coke, 3% Ca(OH)₂ was added into BC to enlarge the characteristics of Ca in MF. As shown in Figure 4, the CRI increases significantly under a CO₂ atmosphere, and

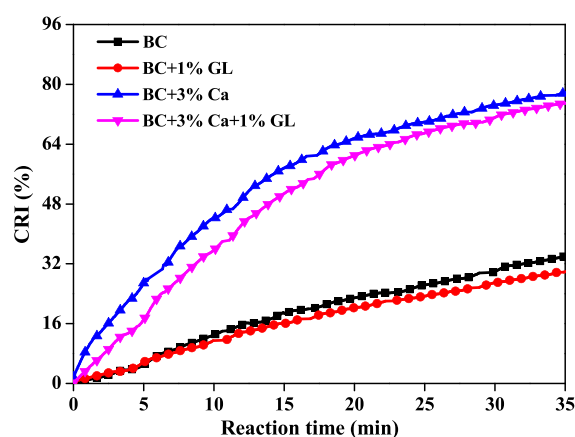


Figure 4. CRI of coke from pyrolysis of BC with Ca and GL.

after adding 1% GL, the CRI decreases, meaning that the catalytic effect of Ca on gasification reactivity of coke is further weakened. The catalytic effect of Ca on the coke gasification reaction needs to meet the following conditions: (1) uniform distribution on the coke surface with a non-sintering form, (2) combination with the active oxygen-containing functional groups in coke, (3) generation of active sites on the coke surface.³³ The addition of GL can transform Ca into stable silicoaluminate and reduce its activity.^{34,35} Also, GL catalyzes

the coal pyrolysis process and increases the release amount of oxygen, leading to the reduction of the number of oxygen-containing functional groups on the coke surface and weakening the catalytic activity of Ca.³⁶ It can be seen that GL can effectively weaken the catalytic effect of Ca on coke reactivity.

Figure 5 shows the microcrystalline structure of coke obtained from pyrolysis with the addition of Ca and GL. It

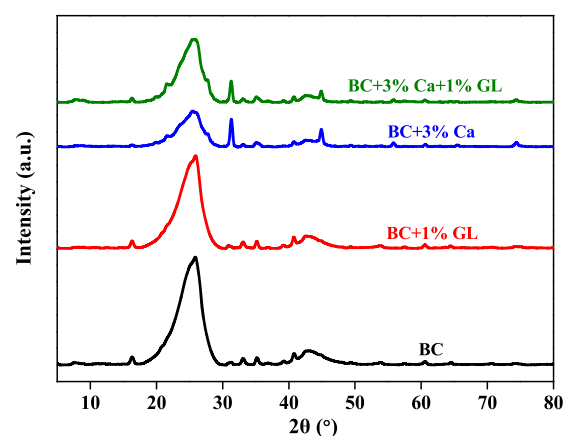


Figure 5. XRD of coke from pyrolysis of BC with Ca and GL.

can be seen that the 002 and 100 peaks are significantly weakened after the addition of Ca, and the 002 peak is intensified after the further addition of GL. The existence of Ca in the pyrolysis process will promote the disorder between the transverse and longitudinal aromatic layer stack and suppress the graphitization of coke.^{37,38} When GL is added, it will bind and transform Ca into a stable state, weakening the combination with the carbon structure and catalytic effect on pyrolysis. Thus, the microcrystalline structure is deteriorated and the reactivity of coke is further reduced.

2.1.3. Ten Kilogram-Scale Coke Oven Amplification Experiment. To better simulate the industrial coking process in a coke oven and verify the influence of GL on the properties of coke, a set of 10 kg-scale tests were carried out. The coke yield, coke reactivity (CRI), and coke strength after reaction (CSR) were measured. As shown in Table 1, the addition of

Table 1. Experimental Data of BC with 0.7% GL in a 10 kg Coke Oven

sample	coke yield (%)	CRI (%)	CSR (%)
BC	69.93	25.02	63.48
BC + 0.7% GL	69.89	22.91	69.34

0.7% GL can effectively reduce the CRI and increase the CSR of the coke. The experimental results prove the effective role of GL in CRI reduction in the subsequent industrial coking experiments. Since the alkali metals are generally circulated in the blast furnace, the improvement effect of GL on the reactivity may be more significant in the blast furnace.

2.2. Effect of Volatiles on Sulfur Transformation during Pyrolysis. **2.2.1. Influence of MF on the Sulfur Removal Rate during Pyrolysis.** Figure 6a shows the changes of the sulfur removal rate and sulfur content in coke with different proportions of MF. It can be seen that when the ratio of MF in coal blends is below 6%, the sulfur removal rate increases and the sulfur content in coke is significantly

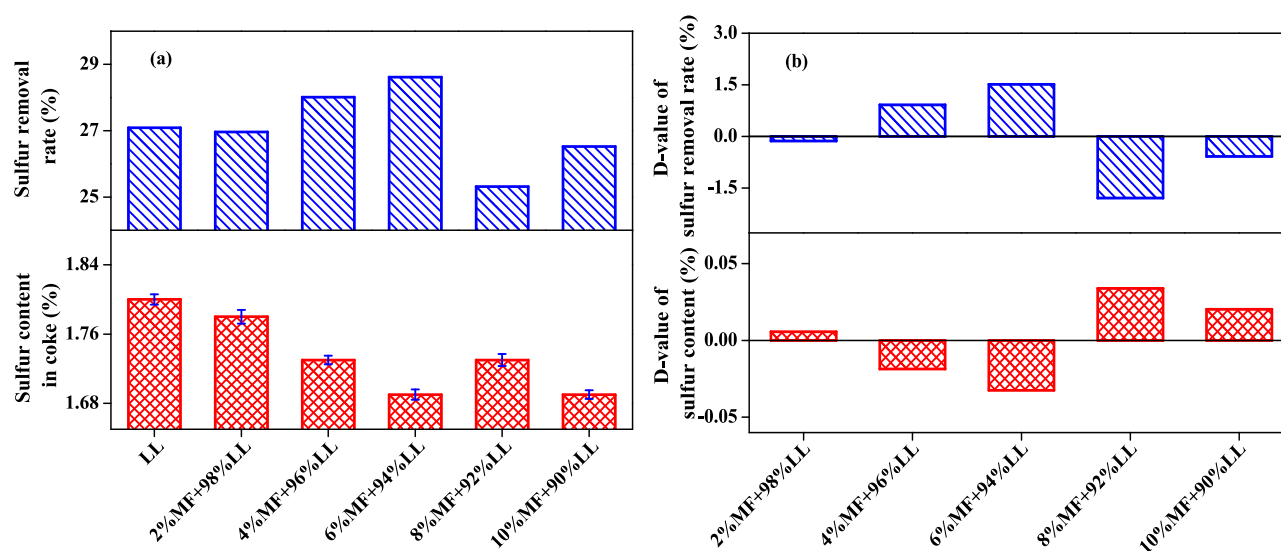


Figure 6. Changes of sulfur content in coke and sulfur removal rate (a) and differences between the experimental and calculated values (b) with different proportions of MF in coal blends.

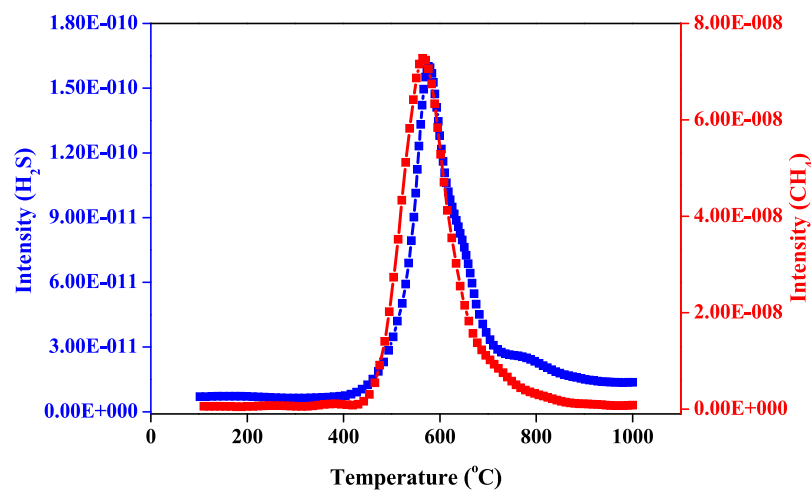


Figure 7. H₂S of LL release curve and CH₄ of MF release curve during co-pyrolysis.

reduced. It is worth noting that there is no absolute linear relationship between the ratio of MF and the sulfur removal rate. When the ratio of MF continues to increase, the sulfur removal rate decreases and the sulfur content in coke slightly increases.

To explore the interaction between MF and LL coal and the influence on sulfur transformation, the differences between the experimental and calculated values of the sulfur content in coke and the sulfur removal rate are calculated and shown in Figure 6b. It can be found that the experimental value of the sulfur removal rate is higher than the calculated value when the ratio of MF is lower, which indicates a better sulfur removal. When the addition ratio further increases, the experimental value becomes lower than the calculated value, indicating that the sulfur fixation effect of MF coal is higher than the sulfur removal effect of volatiles. It can be speculated that there are interactions among different coals in coal blends during pyrolysis, which further influences the conversion of sulfur forms. One of the interactions is beneficial to the sulfur release. A large number of hydrogen-containing free radicals generated from MF can activate the C–S bonds in LL coal,³⁹ promoting the generation of sulfur-containing free radicals and release in

gaseous form. Figure 7 shows the H₂S release curve of LL coal and the CH₄ release curve of MF coal during temperature-programmed pyrolysis. It can be seen that the release temperature range of CH₄ has a good overlap with that of H₂S. CH₄ mainly comes from the decomposition of aliphatic side chains in coal, and the generated hydrogen-containing active groups will further influence the generation of active sulfur and the release of sulfur-containing gas in this temperature zone.⁴⁰ However, another aspect of interaction, that is, the sulfur fixation, also exists. Since MF has a higher content of alkaline minerals (such as calcium and iron) that can capture sulfur-containing free radicals to generate a stable sulfur form, the retention of sulfur in coke occurs when the ratio of MF is further increased.

2.2.2. Influence of GL on the Sulfur Removal Rate of Pyrolysis. Figure 8 shows the sulfur removal rate and sulfur content in coke with different proportions of GL in coal blends. It can be seen that the addition of GL improves the sulfur removal rate and reduces the sulfur content in coke. Here, 0.5% GL has the highest sulfur removal rate and lowest sulfur content in coke. However, with the further increase in GL, the sulfur content in coke slightly increases, indicating that

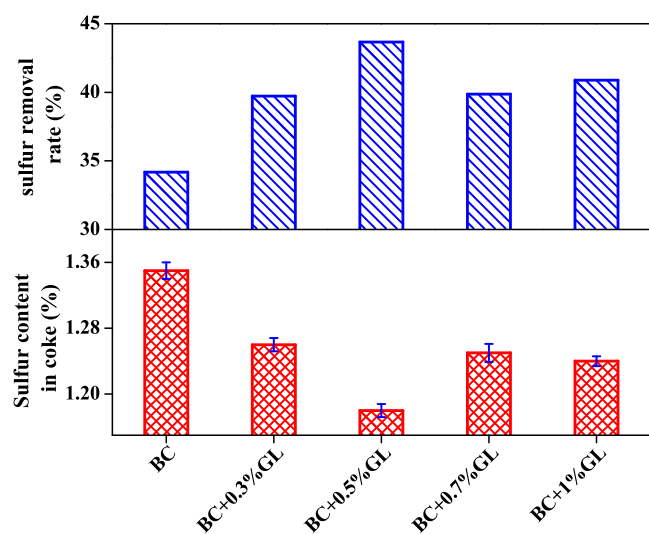


Figure 8. Changes of the sulfur content in coke and sulfur removal rate with different proportions of GL in coal blends.

GL does not have a linear promoting effect on the sulfur transformation behavior during pyrolysis.

Figure 9 shows the thermal weight loss analysis of coal blends with different proportions of GL. The addition of GL increases the thermal weight loss of the coal blends. Moreover, from the DTG curve of the coal blends, it can be seen that the addition of GL widens the volatile release temperature range of coal blends and increases the maximum release rate. Figure S1 indicates that the addition of GL reduces the coke yield, which is consistent with the result of the increase in weight loss of coal blends.

On the one hand, GL can combine with alkaline minerals and reduce the capture of sulfur-containing free radicals. In addition, GL has a certain catalytic effect on the pyrolysis process, which can promote the decomposition of organic matter.⁴¹ Therefore, more hydrogen-containing and oxygen-containing active free radicals can be generated, and the sulfur-containing free radicals generated at higher temperatures can be stabilized and removed from the coke. Moreover, silicon will occupy part of the active sites that can bind sulfur, and the silicon that is not evenly distributed on the coke surface tends to accumulate in the same position as that of sulfur on the coke surface, thus inhibiting the reaction between sulfur and coke.⁴²

However, with the further increase of GL ratio, it can partially hinder the removal of sulfur from coke. As discussed above, the addition of GL reduces the order degree of the coke microcrystalline structure, increases the active carbon atoms on the coke surface, and intensifies the reaction between organic matter and sulfur. During the pyrolysis process, the sulfur-containing radicals may bind with the active sites and remain in the coke. In addition, the further increased GL may block part of the pore structure, affecting the timely removal of sulfur-containing radicals with volatile. Consequently, the possibility of combination of sulfur-containing radicals with organic matter or minerals increases.

To achieve the directional regulation of sulfur content in the pyrolysis process, on the one hand, different forms of sulfur should decompose as much as possible; on the other hand, enough active hydrogen should be supplied for the decomposed sulfur-containing groups to form sulfur-containing gases and release into the gas phase.⁴³ Figure 10 shows the release curves of H₂S and CH₄ during the pyrolysis of BC with different proportions of GL, and the addition of GL promotes the release of H₂S. Figure 11 shows the release curve of COS and CO₂ during the pyrolysis process with different proportions of GL. It can be seen that the addition of GL significantly increases the release of oxygen-containing gases.

When the temperature is higher, the generated sulfur-containing fragments mainly interact with the organic matter and alkaline minerals to form stable thiophene sulfur and inorganic sulfate sulfur and be retained in the coke. The release temperature range of CO₂ overlaps with the release temperature range of COS, indicating that the sulfur free radicals can combine with the active oxygen in the surrounding chemical environment to be released from the coke.

2.2.3. Sulfur Form Analysis of Coke of GL-Added Coal Blends. Table 2 shows the relative proportions of different forms of sulfur on the surface of coke obtained from pyrolysis of GL-added coal blends. It can be seen that the most apparent change in sulfur form is the increase in thiophene sulfur and decrease in sulfate sulfur. When adding 1% GL, the relative proportions of sulfate and thiophene are reduced from 8.10 to 4.45% and increased from 32.36 to 37.05%, respectively.

Thiophene in coke generally has the following sources: the original thiophene in coal that is transferred into the coke and the secondary reaction of sulfur-containing free radical fragments with coal organic matter. The addition of GL

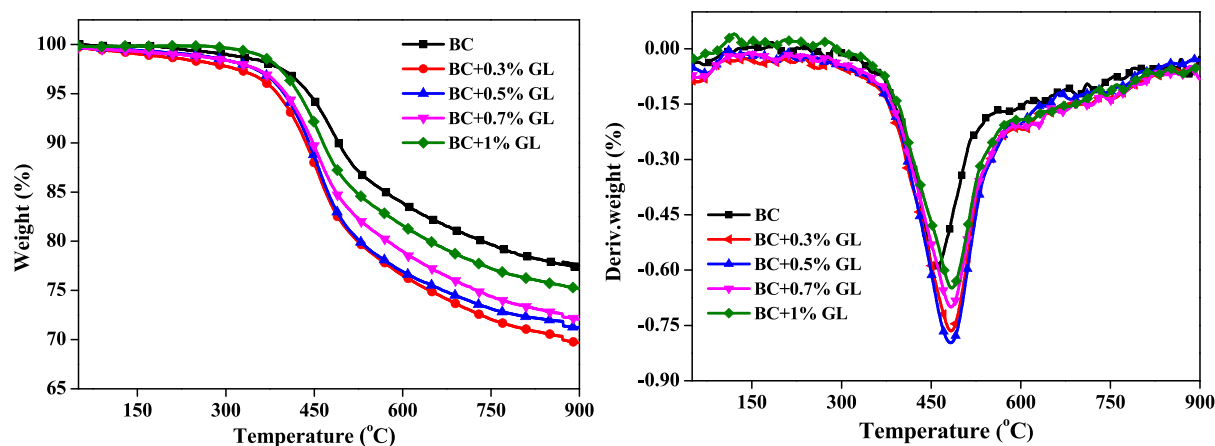


Figure 9. TG and DTG curve of BC with different proportions of GL.

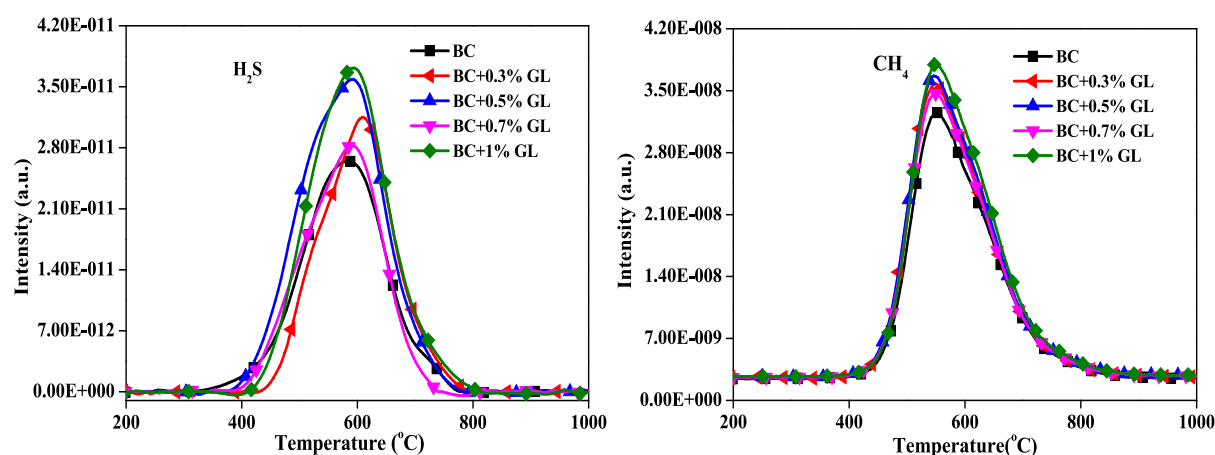


Figure 10. $\text{H}_2\text{S}/\text{CH}_4$ release curve from pyrolysis of BC with different proportions of GL.

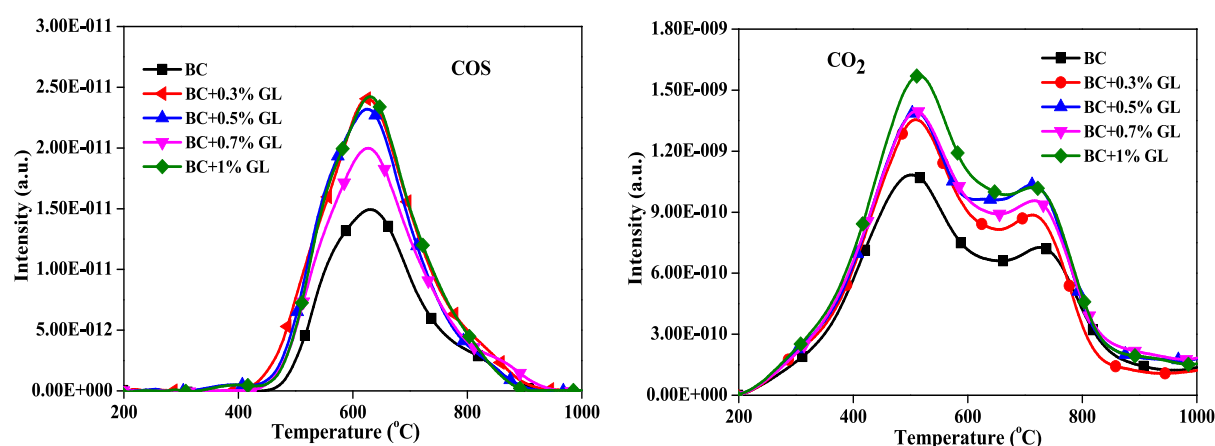


Figure 11. COS/CO_2 release curve from pyrolysis of BC with different proportions of GL.

Table 2. XPS Analysis Data of Coke from Pyrolysis of BC with GL

sample	sulfide-S (%)	thiophene-S (%)	sulfoxide-S (%)	sulfone-S (%)	sulfate-S (%)
BC	6.47	32.36	51.39	1.69	8.10
BC + 1% GL	7.46	37.05	50.50	0.55	4.45

results in the decrease in sulfur content in coke, so the increase in the relative proportion of thiophene sulfur comes from the secondary reaction of sulfur-containing free radical fragments with coal organic matter. As can be seen from Figure 10, GL promotes the formation of hydrogen-containing hydrocarbons during the pyrolysis process. In view of the hydrogen balance, the condensation of semi-coke at a higher temperature is intensified, and the sulfur-containing radicals are easily captured by organic matter. Also, the addition of GL leads to the deterioration of the microcrystalline structure, which increases active carbon atoms on the edge of the coke. This may further increase the capturing probability of the sulfur-containing fragments by organic matter.

Since the coal has undergone heavy-medium sorting and most of the sulfate is removed, the sulfate in coke is mainly formed from the capture of sulfur-containing free radical fragments by alkaline minerals in the long flame coal. As can be seen from Table 2, the content of sulfate sulfur is significantly reduced. It indicates that GL combines with alkaline minerals

at higher temperatures to form stable silicate aluminate, which weakens its capture of sulfur free radicals.

These findings provide a possible approach to reduce the capture ability of sulfur by alkaline minerals through the regulation of interactions between different minerals in coal blends.

3. CONCLUSIONS

In this work, the compatibility of long flame coal and high-sulfur coking coal during co-pyrolysis was studied, and the influence of long flame coal on sulfur removal was explored. A silicon-aluminum-based mineral (GL) that universally exists in coal was selected as coking additives to study the effects on the reactivity of coke and the sulfur transformation behavior during pyrolysis. The conclusions could be summarized as follows:

- (1) GL can effectively reduce the reactivity of coke. The CRI reaches the lowest when 0.7% GL is added in the coal blends. The improvement effect of GL on coke reactivity is verified by a 10 kg coke oven experiment. When the content of alkaline minerals is higher, GL can effectively weaken the destructive effect of alkaline minerals on the graphitization of coke.
- (2) The addition of MF with high volatiles can effectively improve the sulfur removal rate of pyrolysis, and adding 6% MF in the coal blends obtains the highest sulfur removal rate and lowest sulfur content in coke. It proves

Table 3. Analysis Parameters of Samples^a

sample	proximate analysis (wt %)			ultimate analysis (wt %)						
	M _{ad}	A _d	V _{daf}	C _{daf}	H _{daf}	N _{daf}	S _d	O*	G	Y (mm)
LL	0.20	9.76	21.50	88.49	4.69	1.42	1.94	3.25	85.00	16.50
MF	2.34	1.12	38.87	81.96	5.21	1.16	0.16	11.50	10.00	

^aNote: *ad*: air dried basis, *d*: dry basis, *daf*: dry and ash-free basis, *: by difference, *G*: caking index, and *Y*: maximum thickness of the plastic layer.

Table 4. Ash Composition Analyses of Coal Samples^a

sample	ash composition (wt %)										
	SiO ₂	Al ₂ O ₃	Fe ₂ O ₃	CaO	MgO	TiO ₂	SO ₃	K ₂ O	Na ₂ O	P ₂ O ₅	AI
LL	48.70	38.96	4.79	1.80	0.18	1.52	1.16	0.16	0.22	0.72	0.08
MF	34.83	15.70	15.31	18.60	2.95	0.89	8.50	0.16	0.38	0.04	0.74

^aAI = (Fe₂O₃ + CaO + MgO + K₂O + Na₂O)/(SiO₂ + Al₂O₃).

that volatile is an important factor in regulating sulfur transformation behavior during pyrolysis. Sulfur fixation by alkaline minerals deteriorates the sulfur transformation with the further increase of MF in the coal blends.

- (3) The addition of GL in coal blends can effectively improve the sulfur removal rate and reduce the sulfur content in coke, and GL reduces the sulfate sulfur on the surface of the coke, which confirms that GL can combine with alkaline minerals to weaken the capture of sulfur fragments.

4. MATERIALS AND METHODS

4.1. Materials. A high-sulfur coking coal (LL) from Shanxi, China, and the fraction (MF) of a long flame coal from Shanxi, China, with a density less than 1.35 g/cm³ were selected according to a previous study.⁸ Organic heavy liquids with a density less than 1.35 g/cm³ prepared by benzene and carbon tetrachloride were selected to carry out floatation experiments of the long flame coal, and a component with a density less than 1.35 g/cm³ was obtained. Samples were ground and sieved into two different particle sizes, 0.15–0.25 and ≤3 mm, which were used for lab-scale pyrolysis experiments and 10 kg-scale coke oven experiments, respectively. The analysis data of samples are shown in Tables 3 and 4. In Table 4, AI is the alkalinity index, which represents the ability of minerals to capture sulfur-containing free radicals. It can be seen that the contents of CaO and Fe₂O₃ in MF ash are higher, and the alkalinity index is 0.74. Figure S2 shows that the volatile release temperature range of MF partially overlaps with that of LL coal, which indicates the possible interaction between LL and MF. GL is a typical silica-aluminum-based mineral commonly found in coal; through crushing and screening, samples with particle sizes of 0.063–0.075 mm were selected for experiments.

4.2. Pyrolysis Apparatus and Methods. **4.2.1. Crucible Coke Experiments.** A series of crucible coke experiments were designed to study the effects of adding different proportions of GL on the sulfur removal rate and reactivity of coke, and Ca(OH)₂ was added to verify the effect of GL. Then, 20% MF and 80% LL coal were selected as the basis coal (BC) to enlarge the capture of sulfur-containing free radicals and catalysis of coke reactivity by alkaline minerals. Different proportions of GL (*X*%) were added into basic coal blends, and the samples were denoted as BC + *X*%GL. Sixty grams of samples were weighed and placed in a crucible with an inner

diameter of 54 mm. The bulk density of the coal sample was controlled to be 0.75 g/cm³ with a moisture content of 10% by adjusting the height of the sample in the crucible. The crucible was placed in a muffle furnace and heated to 1050 °C with a heating rate of 3 °C/min, and the temperature was kept at 1050 °C for 50 min. The sulfur content and coke reactivity of coke were calculated in a dry ash-free basis to ensure that the experiment data was under the same benchmark.

4.2.2. Coking Experiment by a 10 kg-Scale Coke Oven.

The 10 kg-scale coking experiment was conducted on a tamp-charging coke oven, which was designed to simulate the coking process of an industrial coke oven, and the size of the coal tank was 260 mm × 620 mm (width × height). Briefly, the samples were crushed and sieved into particles ≤3 mm as experimental samples, 10 kg of coal blends were first loaded into the coal tank, and the coal density was maintained at 0.75 g/cm³ by controlling the tamping process. Then, the coal tank was put into the coke oven (pre-heated to 800 °C) and further heated to 1050 °C at 3 °C/min. The coal tank was moved away from the oven after maintaining for 15 h at 1050 °C and cooled to room temperature naturally. The obtained coke was collected for further analysis.

The coke reactivity index (CRI) and coke strength after reaction (CSR) from the 10 kg-scale coke oven were tested according to the Chinese National Standards (GB/T 4000–2017). Briefly, 200 g (± 0.5 g) of sample was reacted with CO₂ at 1100 ± 5 °C for 2 h. After the reaction, the partially gasified coke was weighed and then subjected to the tumble test.

The CRI and CSR were obtained by eqs 1 and 2:

$$\text{CRI}(\%) = \frac{m - m_1}{m} \times 100 \quad (1)$$

$$\text{CSR}(\%) = \frac{m_2}{m_1} \times 100 \quad (2)$$

where *m* is the weight of the coke before the reaction (g), *m*₁ is the weight of the coke after the reaction (g), and *m*₂ is the weight of coke with particle size >10 mm after the tumble test (g).

4.2.3. Lab-Scale Coke Gasification Experiments. Experiments on the effect of GL on CRI were carried out. Crucible coke was mixed with different proportions of GL and sieved to 3–6 mm. A quartz reactor containing 8 g (± 0.001 g) of sample was placed in a vertical furnace and heated to 1100 °C under a N₂ atmosphere and then reacted with CO₂ for 2 h, and the gas flow rate of CO₂ was 200 mL/min. After the experiment, the obtained coke was cooled to room temper-

ature under a N₂ atmosphere. The CRI of coke was calculated by measuring the mass change of coke before and after reaction.

4.2.4. Lab-Scale Coal Pyrolysis Experiments. In these series of experiments, samples with a particle size of 0.15–0.25 mm were selected to study the effect of GL addition on the coal pyrolysis process. A quartz reactor containing 3 g (± 0.001 g) of sample with different proportions of GL was placed in a vertical furnace and heated to 1000 °C under an Ar atmosphere, and the gas flow rate of Ar was 300 mL/min. The gas products (including H₂S, CH₄, COS, and CO₂) during temperature-programmed pyrolysis were detected online by a Hiden QIC-20 mass spectrometer. Before each experiment, Ar was purged to replace the air in the reactor to keep an inert atmosphere. To ensure that the experiment was carried out under the same benchmark, the quantity of the coal blends in the pyrolysis experiment was consistent and the GL was not included in the total mass of the coal blends. The gas release curve was calculated without the GL additive.

To study the effect of MF on the sulfur removal rate and sulfur content in coke, 1 g (± 0.001 g) of sample with different proportions of MF was placed in a porcelain boat. The porcelain boat was placed in the corundum reactor of a horizontal furnace and heated from room temperature to 1000 °C under N₂, and the gas flow rate was 300 mL/min. After reaching the final temperature, the coke sample was cooled to room temperature naturally under the atmosphere of N₂.

4.3. Characterization Methods. **4.3.1. Sulfur Content in the Sample and Sulfur Removal Rate during Pyrolysis.** The sulfur content in coal and coke was measured by an HCS-140 High Frequency Infrared Carbon and Sulfur Analyzer (Shanghai Dekai Instrument Co. Ltd.).

Experimental and calculated sulfur removal rates were obtained by eqs 3 and 4:

$$R_1 = 100 - \frac{Y \times (S_{\text{coke}})_{\text{exp}}}{(S_{\text{coal}})_{\text{exp}}} \quad (3)$$

$$R_2 = 100 - \frac{Y^* \times (S_{\text{coke}})_{\text{cal}}}{(S_{\text{coal}})_{\text{cal}}} \quad (4)$$

where R_1 (R_2) is the experimental (calculated) sulfur removal rate (%), $(S_{\text{coal}})_{\text{exp}}$ ($(S_{\text{coal}})_{\text{cal}}$) is the experimental (calculated) sulfur content in coal (%), $(S_{\text{coke}})_{\text{exp}}$ ($(S_{\text{coke}})_{\text{cal}}$) is the experimental (calculated) sulfur content in coke (%), and Y (Y^*) is the experimental (calculated) coke yield (%).

4.3.2. Sulfur Form Analysis. The sulfur forms on the coke surface were analyzed by ES-CALAB250 X-ray photoelectron spectroscopy (XPS), the power was 200 W, and the vacuum degree of the analysis chamber was 10^{-7} Pa. C 1s (284.6 eV) was used as the standard for correction. The spectra were peak fitted through XPS PEAK41 software.⁴⁴

4.3.3. Carbon Structure Characterization. X-ray diffraction (XRD) was used to estimate the crystallite structure of coke. A Cu K α X-ray source (40 kV, 150 kV) was used. The coke was packed into an aluminum holder and scanned in angular range of 5–90° with a scanning rate of 4 °/min, and the sampling interval was set as 0.02°/step.

4.3.4. Porosity Analysis. The real density of the coke was measured by an AccuPyc 1340 pycnometer. The porosity of coke was calculated by eq 5

$$\varepsilon = \left(1 - \frac{\rho}{d}\right) \times 100\% \quad (5)$$

where ε is the porosity (%), ρ is the bulk density (g/cm³), and d is the real density (g/cm³).

■ ASSOCIATED CONTENT

Supporting Information

The Supporting Information is available free of charge at <https://pubs.acs.org/doi/10.1021/acsomega.1c05642>.

(Figure S1) Coke yields of coal blends with the different proportions of GL and (Figure S2) TG and DTG curves of samples (PDF)

■ AUTHOR INFORMATION

Corresponding Authors

Meijun Wang – State Key Laboratory of Clean and Efficient Coal Utilization, Taiyuan University of Technology, Taiyuan 030024, P.R. China; Key Laboratory of Coal Science and Technology (Taiyuan University of Technology), Ministry of Education, Taiyuan 030024, P.R. China; orcid.org/0000-0002-5558-3536; Email: wangmeijun@tyut.edu.cn

Liping Chang – State Key Laboratory of Clean and Efficient Coal Utilization, Taiyuan University of Technology, Taiyuan 030024, P.R. China; Key Laboratory of Coal Science and Technology (Taiyuan University of Technology), Ministry of Education, Taiyuan 030024, P.R. China; Email: lpchang@tyut.edu.cn

Authors

Wenguang Li – State Key Laboratory of Clean and Efficient Coal Utilization, Taiyuan University of Technology, Taiyuan 030024, P.R. China; Key Laboratory of Coal Science and Technology (Taiyuan University of Technology), Ministry of Education, Taiyuan 030024, P.R. China

Yanfeng Shen – State Key Laboratory of Clean and Efficient Coal Utilization, Taiyuan University of Technology, Taiyuan 030024, P.R. China; Key Laboratory of Coal Science and Technology (Taiyuan University of Technology), Ministry of Education, Taiyuan 030024, P.R. China

Jiang Guo – State Key Laboratory of Clean and Efficient Coal Utilization, Taiyuan University of Technology, Taiyuan 030024, P.R. China; Key Laboratory of Coal Science and Technology (Taiyuan University of Technology), Ministry of Education, Taiyuan 030024, P.R. China

Jiao Kong – State Key Laboratory of Clean and Efficient Coal Utilization, Taiyuan University of Technology, Taiyuan 030024, P.R. China; Key Laboratory of Coal Science and Technology (Taiyuan University of Technology), Ministry of Education, Taiyuan 030024, P.R. China

Complete contact information is available at: <https://pubs.acs.org/doi/10.1021/acsomega.1c05642>

Notes

The authors declare no competing financial interest.

■ ACKNOWLEDGMENTS

The authors gratefully acknowledge the financial support of National Natural Science Foundation of China (U1910201 and 21878208), Shanxi Province Science Foundation for Key Program (201901D111001(ZD)), and Program for the Top

Young Academic Leaders of Higher Learning Institutions of Shanxi.

REFERENCES

- (1) Shen, Y.; Wang, M.; Wu, Y.; Hu, Y.; Kong, J.; Duan, X.; Wang, J.; Chang, L.; Bao, W. Role of gas coal in directional regulation of sulfur during coal-blending coking of high organic-sulfur coking coal. *Energy Fuels* **2020**, *34*, 2757–2764.
- (2) Song, T.; Zhang, J.; Wang, G.; Wang, H.; Xu, R. Effect of lignite addition on gasification properties and coke strength after reaction. *ISIJ Int.* **2018**, *58*, 1218–1223.
- (3) Huang, J.; Yang, Y.; Cao, Y.; Song, L.; Huang, D. Effect of iron particles on the coke solution loss reaction. *ACS Omega* **2020**, *5*, 25042–25048.
- (4) Suzuki, T.; Ohme, H.; Watanabe, Y. Alkali metal catalyzed carbon dioxide gasification of carbon. *Energy Fuels* **1992**, *6*, 343–351.
- (5) Li, K.; Zhang, J.; Barati, M.; Khanna, R.; Liu, Z.; Zhong, J.; Ning, X.; Ren, S.; Yang, T.; Sahajwalla, V. Influence of alkaline (Na, K) vapors on carbon and mineral behavior in blast furnace cokes. *Fuel* **2015**, *145*, 202–213.
- (6) Zhang, Y.; Liang, P.; Jiao, T.; Wu, J.; Zhang, H. Effect of foreign minerals on sulfur transformation in the step conversion of coal pyrolysis and combustion. *J. Anal. Appl. Pyrolysis* **2017**, *127*, 240–245.
- (7) Liu, L.; Fei, J.; Cui, M.; Hu, Y.; Wang, J. XANES spectroscopic study of sulfur transformations during co-pyrolysis of a calcium-rich lignite and a high-sulfur bituminous coal. *Fuel Process. Technol.* **2014**, *121*, 56–62.
- (8) Li, W. G.; Shen, Y. F.; Guo, J.; Kong, J.; Wang, M. J.; Chang, L. P. Effect of flotation fractions of long-flame coal on regulation of sulfur and coke reactivity during pyrolysis of high-sulfur coking coal. *J. Fuel Chem. Technol.* **2021**, *49*, 881–889.
- (9) Zhang, L. X.; Kudo, S.; Tsubouchi, N.; Hayashi, J. I.; Ohtsuka, Y.; Norinaga, K. Catalytic effects of Na and Ca from inexpensive materials on in-situ steam gasification of char from rapid pyrolysis of low rank coal in a drop-tube reactor. *Fuel Process. Technol.* **2013**, *113*, 1–7.
- (10) Berkutov, N. A.; Koshkarov, D. A.; Stepanov, Y. V. Influence of the batch's ash content on coke quality (CRI and CSR). *Coke Chem.* **2013**, *56*, 201–203.
- (11) Karimi, A.; Gray, M. R. Effectiveness and mobility of catalysts for gasification of bitumen coke. *Fuel* **2011**, *90*, 120–125.
- (12) Jensen, P. A.; Frandsen, F. J.; Dam-johansen, K.; Sander, B. Experimental investigation of the transformation and release to gas phase of potassium and chlorine during straw pyrolysis. *Energy Fuels* **2000**, *14*, 1280–1285.
- (13) Keown, D. M.; Favas, G.; Hayashi, J.-I.; Li, C.-Z. Volatilisation of alkali and alkaline earth metallic species during the pyrolysis of biomass: Differences between sugar cane bagasse and cane trash. *Bioresour. Technol.* **2005**, *96*, 1570–1577.
- (14) Wei, X. F.; Huang, J. J.; Liu, T. F.; Fang, Y. T.; Wang, Y. Transformation of alkali metals during pyrolysis and gasification of a lignite. *Energy Fuels* **2008**, *22*, 1840–1844.
- (15) Wang, Y.; Jin, W.; Huang, T.; Zhu, L.; Wu, C.; Yu, G. Characteristics of alkali and alkaline-earth metals for the catalytic gasification of coal char in a fixed-bed reactor. *Energy Technol.* **2013**, *1*, 544–550.
- (16) Ding, L.; Zhang, Y.; Wang, Z.; Huang, J.; Fang, Y. Interaction and its induced inhibiting or synergistic effects during co-gasification of coal char and biomass char. *Bioresour. Technol.* **2014**, *173*, 11–20.
- (17) Mei, Y.; Wang, Z.; Fang, H.; Wang, Y.; Huang, J.; Fang, Y. Na-containing mineral transformation behaviors during Na₂CO₃-Catalyzed CO₂ gasification of high-alumina coal. *Energy Fuels* **2017**, *31*, 1235–1242.
- (18) Habibi, R.; Kopycinski, J.; Masnadi, M. S.; Lam, J.; Grace, J. R.; Mims, C. A.; Hill, J. M. Co-gasification of biomass and non-biomass feedstocks: synergistic and inhibition effects of switchgrass mixed with sub-bituminous coal and fluid coke during CO₂ gasification. *Energy Fuels* **2013**, *27*, 494–500.
- (19) Tran, K.-Q.; Iisa, K.; Steenari, B.-M.; Lindqvist, O. A kinetic study of gaseous alkali capture by kaolin in the fixed bed reactor equipped with an alkali detector. *Fuel* **2005**, *84*, 169–175.
- (20) Zheng, Y.; Jensen, P. A.; Jensen, A. D. A kinetic study of gaseous potassium capture by coal minerals in a high temperature fixed-bed reactor. *Fuel* **2008**, *87*, 3304–3312.
- (21) Escobar, I.; Müller, M. Alkali removal at about 1400 °C for the pressurized pulverized coal combustion combined cycle. 2. sorbents and sorption mechanisms. *Energy Fuels* **2007**, *21*, 735–743.
- (22) Gornostayev, S. S.; Tanskanen, P. A.; Heikkinen, E.-P.; Kerkkonen, O.; Härkki, J. J. An example of alkalization of SiO₂ in a blast furnace coke. *Energy Fuels* **2007**, *21*, 2637–2641.
- (23) Wang, J.; Yao, Y.; Cao, J.; Jiang, M. Enhanced catalysis of K₂CO₃ for steam gasification of coal char by using Ca(OH)₂ in char preparation. *Fuel* **2010**, *89*, 310–317.
- (24) Wang, M.; Liu, Z.; Chu, M.; Shi, Q.; Tang, J.; Han, D.; Cao, L. Influence of temperature and CO₂ on high-temperature behavior and microstructure of metallurgical coke. *ACS Omega* **2021**, *6*, 19569–19577.
- (25) Feroso, J.; Arias, B.; Gil, M. V.; Plaza, M. G.; Pevida, C.; Pis, J. J.; Rubiera, F. Co-gasification of different rank coals with biomass and petroleum coke in a high-pressure reactor for H₂-rich gas production. *Bioresour. Technol.* **2010**, *101*, 3230–3235.
- (26) Jiao, H.; Wang, M.; Kong, J.; Yan, D.; Guo, J.; Chang, L. Contribution of single coal property to the changes of structure and reactivity of chars from blending coking. *J. Anal. Appl. Pyrolysis* **2018**, *134*, 114–121.
- (27) Gong, X.; Zhang, S. Changes in char structure due to inorganic matters during anthracite pyrolysis. *J. Anal. Appl. Pyrolysis* **2017**, *127*, 170–175.
- (28) Huang, J.; Tao, L.; Tie, W.; Li, Z.; Wang, Q.; Liu, Z. Transport properties of CO₂ in different reactivity coke solution loss reaction based on stefan flow theory. *ACS Omega* **2020**, *5*, 26817–26828.
- (29) Numazawa, Y.; Hara, Y.; Matsukawa, Y.; Matsushita, Y.; Aoki, H.; Shishido, T.; Okuyama, N. Kinetic modeling of CO₂ and H₂O gasification reactions for metallurgical coke using a distributed activation energy model. *ACS Omega* **2021**, *6*, 11436–11446.
- (30) Guo, W.-T.; Xue, Q.-G.; Ling, C.; Zuo, H.-B.; Wang, J.-S.; Han, Y.-H. Influence of pore structure features on the high temperature tensile strength of coke. *J. Eng. Sci.* **2016**, *7*, 930–936.
- (31) Komarova, E.; Guhl, S.; Meyer, B. Brown coal char CO₂-gasification kinetics with respect to the char structure. Part I: Char structure development. *Fuel* **2015**, *152*, 38–47.
- (32) Cuiping, W.; Hao, Y.; Yanbo, Y.; Wenzheng, L.; Shirui, Y.; Weiwei, C.; Fengyin, W.; Hongcun, B.; Xiude, H. Chemical looping reforming of coal tar vapor on the surface of CaO-modified Fe-based oxygen carrier. *Energy Fuels* **2020**, *34*, 8534–8542.
- (33) Lang, R. J.; Neavel, R. C. Behavior of calcium as a steam gasification catalyst. *Fuel* **1982**, *61*, 620–626.
- (34) Jin, B.; Wen, L.; Li, C.-Z.; Bai, Z.-Q.; Li, B.-Q. Influence of coal blending on mineral transformation at high temperatures. *Min. Sci. Technol.* **2009**, *19*, 300–305.
- (35) Jiang, M. Q.; Zhou, R.; Hu, J.; Wang, F. C.; Wang, J. Calcium-promoted catalytic activity of potassium carbonate for steam gasification of coal char: Influences of calcium species. *Fuel* **2012**, *64*–71.
- (36) Hadi, B.; Sokoto, A. M.; Garba, M. M.; Muhammad, A. B. Effect of neat kaolin and CuO/Kaolin on the yield and composition of products from pyrolysis of polystyrene waste. *Energy Sources, Part A* **2017**, *39*, 148–153.
- (37) Feng, B.; Bhatia, S. K.; Barry, J. C. Structural ordering of coal char during heat treatment and its impact on reactivity. *Carbon* **2002**, *40*, 481–496.
- (38) Zhang, J.; Zhang, R.; Bi, J. Effect of catalyst on coal char structure and its role in catalytic coal gasification. *Catal. Commun.* **2016**, *79*, 1–5.
- (39) Wang, H.; Feng, Y.; Zhang, X.; Lin, W.; Zhao, Y. Study of coal hydrolysis and desulfurization by ReaxFF molecular dynamics simulation. *Fuel* **2015**, *45*, 241–248.

(40) Shen, Y.; Wang, M.; Hu, Y.; Kong, J.; Wang, J.; Chang, L.; Bao, W. Transformation and regulation of sulfur during pyrolysis of coal blend with high organic-sulfur fat coal. *Fuel* **2019**, *249*, 427–433.

(41) Meng, F.; Gupta, S.; Yu, J.; Jiang, Y.; Koshy, P.; Sorrell, C.; Shen, Y. Effects of kaolinite addition on the thermoplastic behavior of coking coal during low temperature pyrolysis. *Fuel Process. Technol.* **2017**, *167*, 502–510.

(42) Zhou, S.; Yang, J.; Liu, Z.; Yan, J. Influence of silicon on uptake of H₂S by a coke under elevated temperature. *J. Anal. Appl. Pyrolysis* **2009**, *84*, 165–169.

(43) Zhang, Y.; Wang, M.; Qin, Z.; Yang, Y.; Fu, C.; Feng, L.; Chang, L. Effect of the interactions between volatiles and char on sulfur transformation during brown coal upgrade by pyrolysis. *Fuel* **2013**, *103*, 915–922.

(44) Liu, F.; Li, W.; Chen, H.; Li, B. Uneven distribution of sulfurs and their transformation during coal pyrolysis. *Fuel* **2007**, *86*, 360–366.